Electronic Supplementary Material (ESI) for Nanoscale.

Exploring the Mechanisms of Drug-Delivery by Decorated ZnO Nanoparticles through Predictive ReaxFF Molecular Dynamics Simulations

Cheherazade Trouki[a], Giovanni Barcaro[a] and Susanna Monti[b]*

Other Computational Details

MD simulations with AMBER. The average volume of the water simulation box was approximately 405000 Å^3 and contained 14000 water molecules. The average volume of the ethanol simulation box was approximately 202000 Å^3 and contained 1100 ethanol molecules.

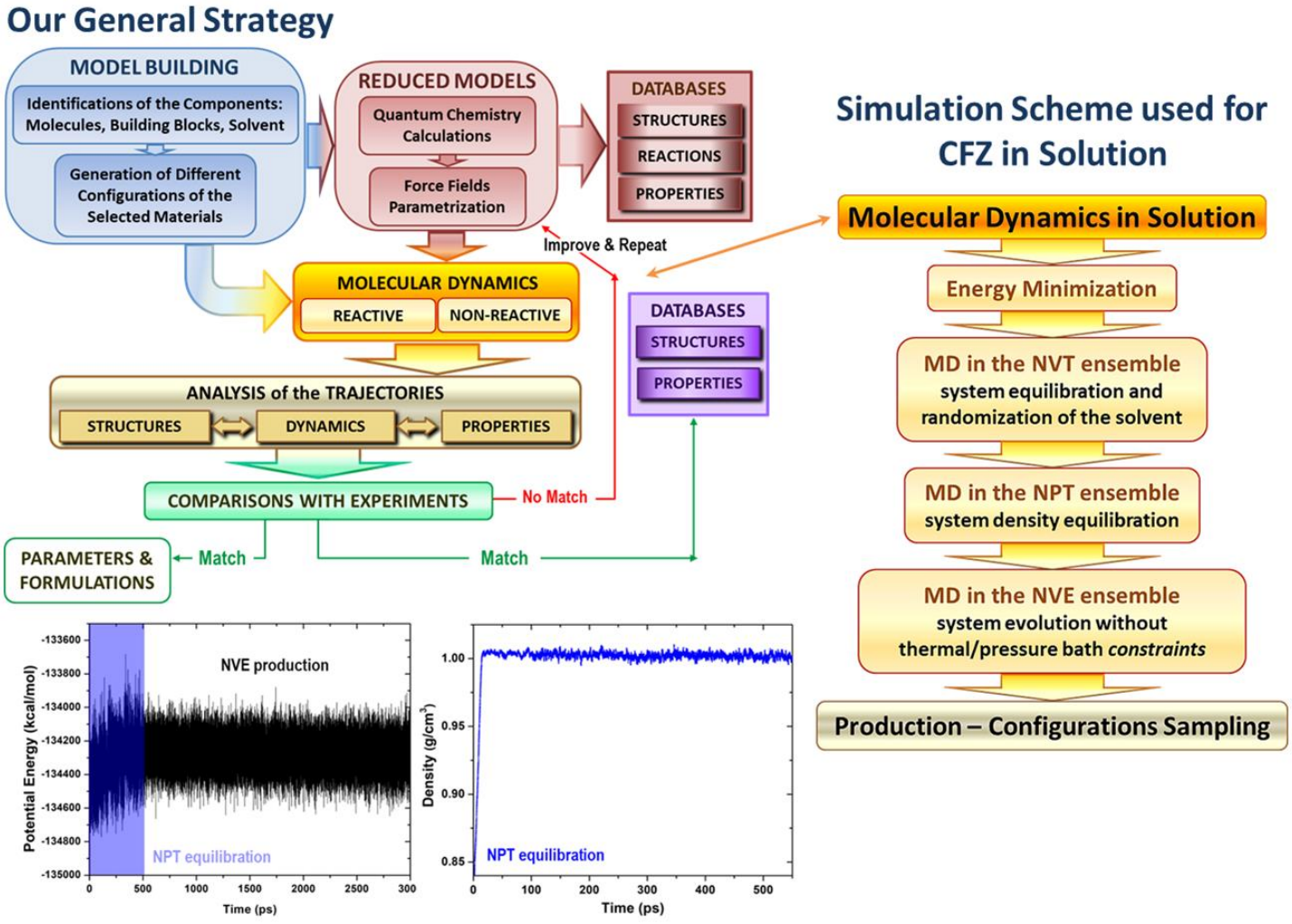

Computational scheme. At the bottom of the scheme, the potential energy trend during the equilibration of CFZ in water solution in the NPT ensemble, and the production phase in the NVE ensemble is shown on the left. On the right, the evolution of the density (water box) during the NPT equilibration is displayed.

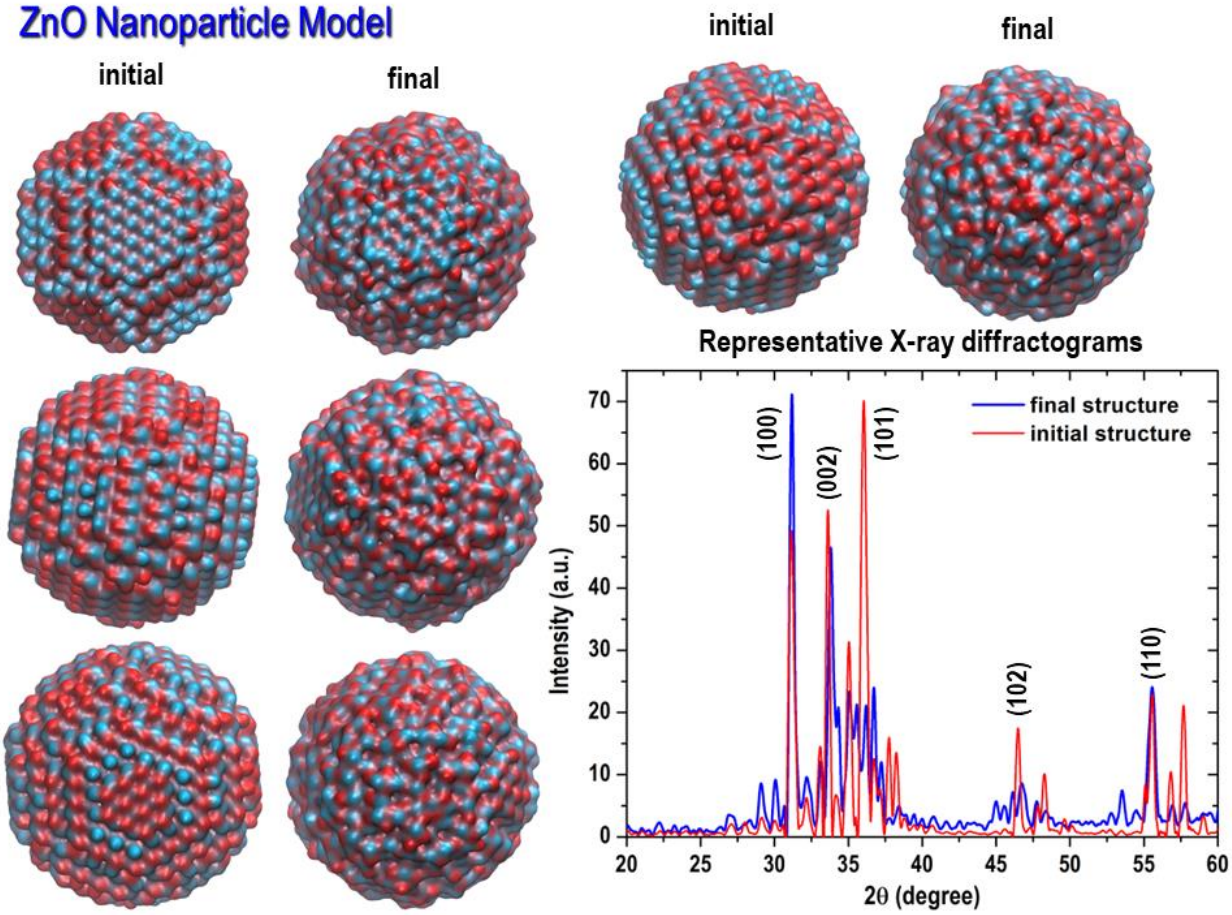

Figure S1 Different views of the initial ZnONP model after construction and its final equilibrated structure. Calculated diffractograms of the initial and final geometries with the characteristic reflections (slightly shifted) of single-phase wurtzite ZnONPs at 2θ = 32, 34, 36, 47, and 57 degrees. Color codes: Zn bluish, O red.

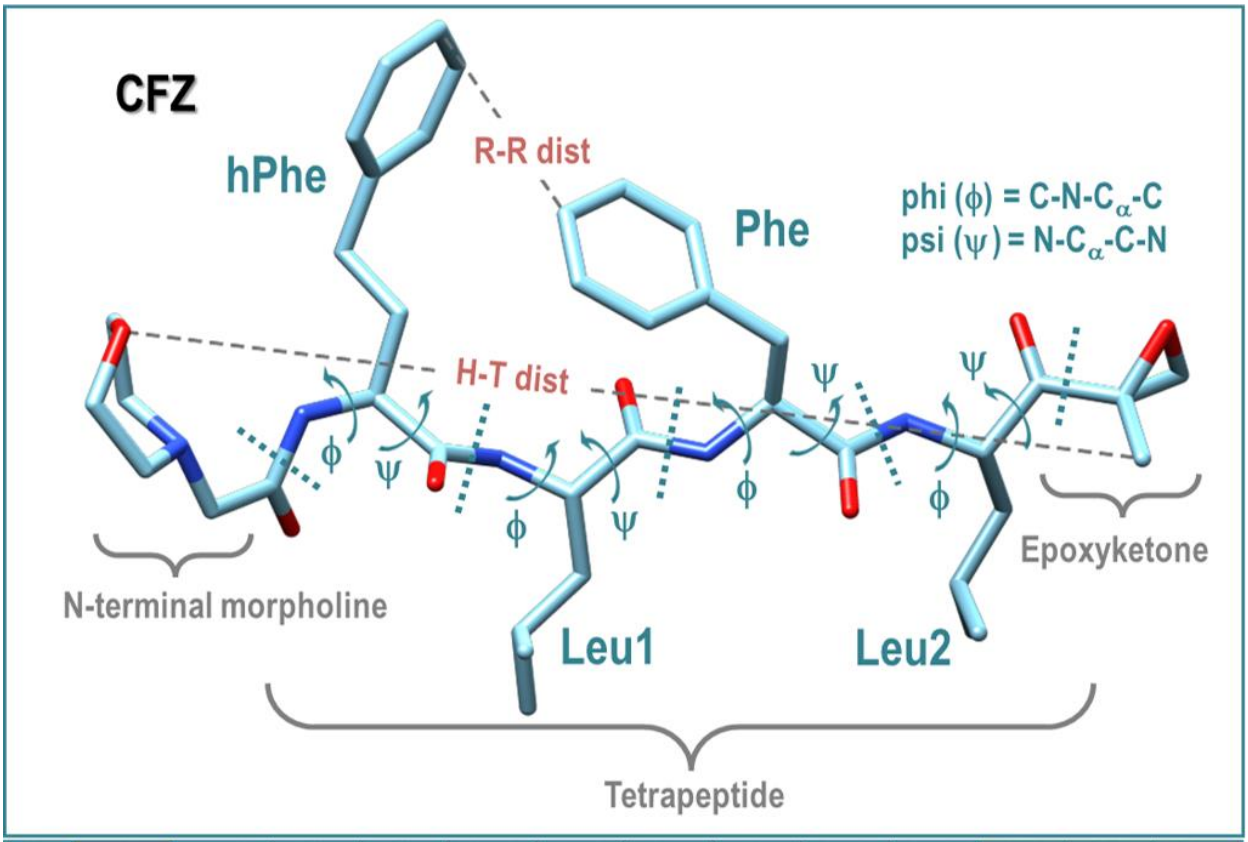

Mol.	ΔE	morph	hPhe phi	hPhe psi	Leu1 phi	Leu1 psi	Phe phi	Phe psi	Leu2 phi	Leu2 psi	H-T dist	R-R dist	R_{gyr}
#	kcal/mol	deg	deg	deg	deg	deg	deg	deg	deg	deg	Å	Å	Å
1	0.0	19.1	-80.2	75.2	-83.9	66.2	-90.8	67.7	-81.9	142.6	15.7	4.8	5.9
2	2.5	90.2	-153.1	170.9	-81.1	58.8	-178.8	174.5	-96.9	126.2	3.8	5.7	5.2
3	3.1	15.9	-65.2	164.9	-78.7	78.5	-80.6	67.2	-79.1	143.7	13.4	4.7	5.7
4	3.4	-28.1	-144.3	178.2	-82.4	111.0	-78.0	78.2	-126.5	71.4	12.1	6.8	5.2
5	3.9	21.6	177.4	162.1	-54.5	150.4	-85.6	80.1	-71.4	144.3	11.8	10.2	5.2
6	5.7	90.5	-153.8	164.9	-83.6	60.2	176.8	149.4	-134.9	152.5	7.1	4.8	5.2
7	6.7	24.3	-148.3	160.2	-100.6	138.1	-167.9	172.6	-56.5	148.6	11.1	4.6	5.9
8	7.8	93.5	-155.0	155.8	-72.1	92.5	-55.9	131.8	-111.7	118.4	10.9	4.5	5.4
9	7.8	21.3	-169.5	154.5	-102.7	177.1	-52.4	132.0	-110.2	123.6	15.1	9.9	5.8
10	8.1	19.3	-149.7	162.2	-83.3	57.3	-168.3	165.8	-50.9	126.1	4.9	5.8	5.3
11	8.3	129.8	-168.7	173.6	-75.4	100.6	-80.0	56.7	-67.3	149.2	14.4	6.4	5.6
12	8.6	21.3	-145.7	161.2	-133.4	169.5	-147.5	159.5	-137.5	159.4	16.6	3.9	6.4
13	8.7	22.9	-145.7	160.3	-133.1	169.0	-148.0	153.9	-140.8	159.0	16.7	3.9	6.4
14	8.7	21.2	-144.8	161.5	-134.4	163.9	-165.4	147.6	-134.2	152.7	16.1	9.7	6.6
15	8.7	20.8	-144.7	161.7	-134.6	164.5	-165.1	147.6	-134.3	152.7	16.2	9.8	6.6
16	9.6	21.6	-152.0	155.6	-88.5	87.1	-157.4	144.4	-134.4	159.8	10.8	3.9	5.6
17	9.7	20.8	-146.8	158.6	-136.8	170.8	-141.3	23.3	-63.3	148.0	16.2	3.9	6.2
18	9.7	170.0	-79.7	81.1	-86.2	64.2	-91.8	70.5	-131.2	62.4	15.3	4.8	5.8
19	9.9	88.0	-153.7	160.3	-129.9	170.2	-146.2	151.5	-64.4	150.7	16.4	3.9	6.5
20	10.0	22.3	-144.2	158.1	-142.2	158.3	-86.5	129.7	-110.9	136.3	16.3	13.5	6.5
21	10.0	87.9	-153.8	160.2	-132.2	171.0	-147.4	154.0	-62.2	150.6	16.5	3.9	6.5

Figure S2 CFZ conformers within 10 kcal/mol of the minimum energy structure. The geometries have been obtained through Balloon conformational search and optimized at the DFT M06-2X/6-31G(d) level in the gas phase. Morph = N-C-C-N dihedral angle, phi and psi dihedral angles (degrees = deg) of all the residues (hPhe, Leu1, Phe, Leu2), Head-Tail, Ring-Ring distances (Å), and Radius of gyration (Å).

Mol.	ΔE	morf	hPhe phi	hPhe psi	Leu1 phi	Leu1 psi	Phe phi	Phe psi	Leu2 phi	Leu2 psi	H-T	R-R	R_{gyr}
#	kcal/mol	deg	deg	deg	deg	deg	deg	deg	deg	deg	Å	Å	Å
1	0.0	19.1	-80.2	75.2	-83.9	66.2	-90.8	67.7	-81.9	142.6	15.7	4.8	5.9
2	2.5	90.2	-153.1	170.9	-81.1	58.8	-178.8	174.5	-96.9	126.2	3.8	5.7	5.2
3	3.1	15.9	-65.2	164.9	-78.7	78.5	-80.6	67.2	-79.1	143.7	13.4	4.7	5.7
4	3.4	-28.1	-144.3	178.2	-82.4	111.0	-78.0	78.2	-126.5	71.4	12.1	6.8	5.2
5	3.9	21.6	177.4	162.1	-54.5	150.4	-85.6	80.1	-71.4	144.3	11.8	10.2	5.2
6	5.7	90.5	-153.8	164.9	-83.6	60.2	176.8	149.4	-134.9	152.5	7.1	4.8	5.2
7	6.7	24.3	-148.3	160.2	-100.6	138.1	-167.9	172.6	-56.5	148.6	11.1	4.6	5.9
8	7.8	93.5	-155.0	155.8	-72.1	92.5	-55.9	131.8	-111.7	118.4	10.9	4.5	5.4
9	7.8	21.3	-169.5	154.5	-102.7	177.1	-52.4	132.0	-110.2	123.6	15.1	9.9	5.8
10	8.1	19.3	-149.7	162.2	-83.3	57.3	-168.3	165.8	-50.9	126.1	4.9	5.8	5.3
11	8.3	129.8	-168.7	173.6	-75.4	100.6	-80.0	56.7	-67.3	149.2	14.4	6.4	5.6
12	8.6	21.3	-145.7	161.2	-133.4	169.5	-147.5	159.5	-137.5	159.4	16.6	3.9	6.4
13	8.7	22.9	-145.7	160.3	-133.1	169.0	-148.0	153.9	-140.8	159.0	16.7	3.9	6.4
14	8.7	21.2	-144.8	161.5	-134.4	163.9	-165.4	147.6	-134.2	152.7	16.1	9.7	6.6
15	8.7	20.8	-144.7	161.7	-134.6	164.5	-165.1	147.6	-134.3	152.7	16.2	9.8	6.6
16	9.6	21.6	-152.0	155.6	-88.5	87.1	-157.4	144.4	-134.4	159.8	10.8	3.9	5.6
17	9.7	20.8	-146.8	158.6	-136.8	170.8	-141.3	23.3	-63.3	148.0	16.2	3.9	6.2
18	9.7	170.0	-79.7	81.1	-86.2	64.2	-91.8	70.5	-131.2	62.4	15.3	4.8	5.8
19	9.9	88.0	-153.7	160.3	-129.9	170.2	-146.2	151.5	-64.4	150.7	16.4	3.9	6.5
20	10.0	22.3	-144.2	158.1	-142.2	158.3	-86.5	129.7	-110.9	136.3	16.3	13.5	6.5
21	10.0	87.9	-153.8	160.2	-132.2	171.0	-147.4	154.0	-62.2	150.6	16.5	3.9	6.5
22	10.2	82.5	-150.8	167.1	-75.4	80.9	-78.9	73.9	-120.4	166.0	14.5	5.7	5.8
23	10.2	20.3	-144.9	161.4	-138.7	158.6	-86.1	66.8	-87.0	141.7	16.0	7.9	6.0
24	10.2	87.4	-153.3	160.5	-131.3	168.9	-147.0	159.3	-137.7	159.5	17.2	3.9	6.5
25	10.3	87.5	-153.1	160.5	-129.8	170.6	-145.7	151.9	-142.7	159.9	17.3	3.9	6.5
26	10.4	18.7	-61.2	158.4	-132.9	166.7	-148.9	158.5	-137.2	159.3	17.7	3.9	6.5
27	10.6	18.0	-59.6	144.3	-146.5	154.7	-83.7	64.7	-78.8	144.6	16.8	8.6	6.1
28	10.7	-105.1	-65.1	113.8	-94.3	28.3	-82.5	88.5	-122.9	66.2	12.1	6.1	5.3
29	10.8	16.1	-61.0	143.8	-147.7	154.4	-77.7	127.4	-109.1	133.7	17.2	15.0	6.5
30	11.0	21.1	-144.6	161.6	-134.5	164.2	-165.2	146.5	-136.9	158.3	16.2	9.9	6.6
31	11.3	-93.1	-76.1	83.0	-85.4	65.1	-93.4	68.0	-142.3	166.6	13.4	4.8	5.8
32	11.9	80.2	-146.9	136.4	-85.8	54.4	-89.1	74.5	-129.7	67.4	14.6	4.3	5.7
33	11.9	79.0	-146.7	134.7	-85.8	54.3	-89.1	74.2	-129.6	67.3	14.6	4.3	5.7
34	11.9	21.1	-145.2	161.9	-133.9	169.7	-147.6	157.5	-141.3	168.5	16.8	3.9	6.4
35	11.9	22.9	-145.1	162.2	-134.5	168.4	-146.2	158.3	-141.4	168.2	16.7	3.9	6.4
36	12.0	19.9	-80.9	77.6	-144.0	150.3	-77.2	88.7	-160.2	137.7	13.5	17.3	6.2
37	12.1	-114.3	-64.1	133.0	-114.6	18.1	-79.9	80.7	-126.1	67.2	12.8	6.4	5.4
38	12.3	88.6	-151.8	156.5	-110.6	156.6	-166.2	147.9	-135.0	151.7	15.5	8.2	6.5
39	12.3	-27.1	-131.6	167.4	-142.2	155.0	-58.2	141.8	-134.5	156.0	15.5	13.2	6.3
40	12.3	88.4	-151.3	152.1	-139.0	161.2	-165.9	146.1	-136.9	157.0	17.5	11.2	6.8
41	12.3	-26.2	-130.8	167.3	-141.7	153.9	-58.9	141.7	-134.1	155.9	15.6	13.1	6.3
42	12.5	88.1	-152.5	152.4	-110.1	124.5	-86.8	80.6	-123.3	58.1	14.3	4.6	5.8
43	12.6	-179.4	-142.0	164.4	-112.1	18.1	-164.6	178.9	-117.1	74.2	13.4	8.3	5.8
44	12.7	-124.5	-84.0	50.4	-144.0	-139.6	-82.1	73.9	-56.8	130.7	4.1	15.0	5.6
45	12.7	78.4	-152.2	150.7	-89.3	49.6	-122.7	143.2	-142.0	158.9	11.4	5.7	5.7
46	12.8	88.2	-153.9	157.0	-104.9	169.1	-142.3	153.0	-141.8	159.1	16.3	4.5	6.3
47	12.9	144.6	-161.7	153.9	-134.2	167.4	-164.1	147.1	-134.3	153.4	19.7	9.1	6.9
48	13.1	17.7	-59.0	149.6	-143.1	160.1	-160.1	166.5	-117.6	80.8	16.4	11.8	6.7
49	13.4	156.7	-142.4	165.4	-134.1	164.3	-145.5	157.2	-141.0	159.8	20.2	3.8	6.7
50	13.4	84.5	-148.8	157.1	-141.8	159.3	-94.4	133.5	-110.4	128.9	17.9	14.9	6.7
51	13.5	20.8	-79.5	80.9	-143.9	152.0	-78.7	88.4	-144.8	165.4	14.2	16.9	6.2
52	13.5	-146.8	-59.5	154.4	-135.8	164.2	-149.6	153.3	-62.4	151.0	14.8	4.0	6.3
53	13.5	-105.0	-69.1	105.1	-86.6	76.8	-77.8	82.0	-135.6	164.7	12.2	3.9	5.7
54	13.5	87.9	-153.6	160.8	-130.6	168.7	-146.4	157.5	-140.3	168.5	17.2	3.9	6.5
55	13.6	-144.0	-59.5	153.4	-135.8	166.2	-149.4	151.4	-63.0	151.1	14.9	4.0	6.3
56	13.6	87.8	-153.8	160.9	-131.0	169.5	-147.0	155.8	-141.1	169.2	17.2	3.9	6.5
57	13.6	17.8	-61.8	157.7	-131.5	166.8	-148.9	153.8	-141.6	167.9	17.8	3.9	6.5
58	13.7	17.6	-61.3	158.4	-133.5	164.0	-147.0	155.5	-140.7	168.5	17.8	4.0	6.5
59	13.7	-143.8	-58.3	152.5	-135.0	166.5	-149.5	151.4	-63.1	151.1	14.9	4.0	6.3
60	13.7	89.0	-151.1	153.5	-141.4	157.4	-54.8	141.2	-133.4	156.0	17.3	14.1	6.5
61	13.8	153.8	-161.9	174.0	-99.8	131.8	-80.6	83.0	-140.9	164.8	16.8	6.2	5.9

62	13.8	89.2	-151.2	153.5	-140.3	156.4	-55.9	141.2	-134.9	155.7	17.3	13.8	6.5
63	14.1	89.1	-150.8	150.6	-140.3	162.3	-83.3	90.9	-125.1	67.9	15.4	11.8	6.3
64	14.2	88.6	-151.0	155.8	-139.3	162.6	-79.7	89.5	-124.3	66.9	15.5	12.2	6.3
65	14.3	-25.7	-129.6	164.5	-141.0	157.3	-60.1	156.3	-119.6	85.4	14.4	12.1	6.2
66	14.5	166.7	-140.6	161.9	-141.6	155.2	-85.0	65.3	-80.5	143.8	17.7	7.7	6.2
67	14.7	163.9	-140.3	164.0	-139.6	160.5	-85.9	69.0	-92.6	140.6	17.6	8.4	6.2
68	14.8	-126.6	-84.8	80.6	-120.2	177.8	-79.7	61.3	-62.2	148.4	10.3	12.1	5.8
69	14.8	89.6	-150.8	144.5	-99.4	-7.4	-133.6	118.7	-128.9	164.4	10.0	11.3	5.4
70	15.0	-144.5	-61.1	158.8	-136.2	-82.7	-51.3	144.3	-113.8	109.6	14.0	13.0	5.6
71	15.0	132.9	-170.1	174.1	-76.2	88.7	-62.6	148.0	-122.3	166.7	13.9	6.7	5.6
72	15.1	-25.0	-160.0	148.1	-70.6	151.2	-138.4	153.0	-128.5	166.1	14.4	4.9	6.0
73	15.2	157.0	-142.7	151.5	-104.6	-14.0	-144.1	145.8	-117.1	150.4	14.5	12.0	5.9
74	15.3	147.0	-145.9	165.7	-93.0	-1.4	-79.2	91.1	-140.7	165.2	14.5	6.0	5.5
75	15.3	87.8	-153.6	161.6	-130.9	167.6	-145.5	164.8	-125.0	62.5	15.8	3.9	6.3
76	15.3	-132.8	-58.6	148.6	-99.1	-153.1	-74.7	95.3	-129.7	62.4	14.9	10.0	5.7
77	15.3	150.7	-144.0	150.5	-115.4	122.4	-88.6	64.8	-65.9	149.7	18.2	4.5	6.2
78	15.5	-155.5	-83.5	72.9	-124.7	146.6	-151.6	148.5	-140.9	158.9	14.7	7.1	6.4
79	15.5	87.4	-172.9	153.6	-66.6	152.6	-138.8	156.5	-120.9	33.1	12.7	5.0	5.7
80	15.5	-146.8	-83.9	71.9	-128.3	149.8	-152.5	151.8	-59.1	141.5	13.9	7.3	6.5
81	15.7	88.9	-152.1	156.1	-136.9	157.6	-60.0	153.7	-118.4	88.8	16.7	12.2	6.4
82	15.8	87.0	-156.2	168.5	-134.7	-77.9	-51.0	149.9	-122.8	71.5	9.6	12.8	5.4
83	15.8	156.6	-143.3	164.7	-136.3	-83.1	-53.1	148.0	-105.7	132.5	12.0	13.2	5.7
84	15.8	153.6	-143.1	164.2	-136.2	-83.0	-52.2	147.6	-106.2	126.5	12.0	13.1	5.7
85	15.8	87.6	-154.3	160.2	-130.7	168.5	-146.0	156.3	-126.5	72.3	15.9	3.9	6.3
86	16.3	88.8	-151.6	155.4	-137.7	157.1	-85.7	75.2	-146.5	165.7	15.6	7.6	6.1
87	16.4	89.1	-150.7	153.0	-140.5	158.9	-85.4	75.9	-143.2	165.3	15.7	7.9	6.2
88	16.6	-145.4	-57.3	148.4	-145.9	152.8	-60.4	141.5	-134.3	155.9	14.7	14.6	6.3
89	16.6	-145.0	-58.7	149.5	-146.8	154.4	-56.8	141.3	-134.4	156.0	14.7	14.6	6.3
90	16.7	87.8	-154.7	158.8	-110.4	170.5	-142.9	147.6	-127.6	71.7	15.2	4.5	6.1
91	16.7	-101.5	-68.1	108.8	-98.1	5.6	-74.6	89.5	-143.4	164.5	11.0	10.9	5.6
92	16.8	87.5	-154.4	160.0	-130.3	168.5	-143.4	145.7	-128.9	70.0	16.1	3.9	6.2
93	16.9	161.5	-142.8	157.5	-128.9	125.1	-89.3	75.0	-128.2	68.5	17.3	4.4	6.1
94	17.0	87.0	-152.2	161.6	-117.1	165.9	-162.7	164.2	-117.3	86.7	14.7	9.0	6.6
95	17.0	-24.8	-174.4	168.3	-105.2	160.1	-136.1	133.5	-128.5	70.6	15.5	4.9	5.9
96	17.1	115.9	-166.4	173.0	-106.9	169.7	-126.3	115.4	-135.0	164.7	17.2	4.8	6.0
97	17.2	163.4	-140.9	167.0	-134.3	162.5	-80.6	89.4	-124.2	66.7	17.2	10.8	6.3
98	17.5	161.4	-140.5	162.8	-143.0	163.7	-118.1	139.1	-125.4	151.0	19.7	12.6	6.9
99	17.5	-94.8	-55.0	120.7	-155.6	156.9	-78.6	87.2	-140.1	164.9	12.8	10.6	5.8
100	17.5	86.6	-155.5	155.3	-80.8	62.5	-68.9	167.3	-48.4	137.3	12.4	4.6	5.8
101	17.8	154.8	-143.3	163.2	-134.4	166.3	-145.1	146.6	-131.8	165.6	20.2	3.8	6.7
102	17.9	163.2	-143.1	163.4	-137.8	167.4	-147.8	145.2	-123.9	56.7	19.0	3.9	6.5
103	17.9	21.4	-144.6	158.9	-138.1	161.5	-55.4	141.1	-125.2	69.6	16.0	10.2	6.0
104	18.0	85.5	-150.6	158.5	-90.8	-146.7	-80.0	81.5	-126.2	161.5	10.0	12.7	5.5
105	18.2	-32.8	-59.4	146.5	-144.9	154.0	-70.1	141.1	-130.6	164.8	16.6	9.2	6.2
106	18.2	164.8	-141.3	165.5	-133.8	164.1	-145.3	154.8	-129.4	166.3	20.2	3.8	6.7
107	18.3	-152.0	-84.1	72.2	-133.0	141.7	-82.5	84.1	-126.2	65.8	10.2	9.8	5.8
108	18.3	169.2	-140.5	166.0	-136.6	159.6	-85.2	77.3	-129.7	62.1	16.8	8.7	6.1
109	18.4	-130.8	-83.6	84.1	-112.4	155.1	-57.5	145.2	-135.8	145.4	12.5	15.4	6.3
110	18.5	170.0	-140.9	163.6	-137.6	159.7	-58.8	154.2	-118.8	88.2	17.8	11.7	6.4
111	19.0	-143.7	-58.8	149.9	-145.5	159.0	-83.6	78.2	-141.6	164.9	14.0	8.8	5.9
112	19.1	166.4	-141.2	161.9	-139.3	158.6	-85.9	76.2	-128.8	67.9	16.8	8.2	6.2
113	19.1	84.3	-155.1	161.2	-136.5	149.4	-144.8	157.4	-53.9	132.8	15.2	4.5	6.6
114	19.2	90.7	-148.8	162.6	-60.6	165.8	-50.7	147.7	-125.5	70.0	13.0	13.6	5.7
115	19.3	163.3	-141.4	164.9	-136.2	163.0	-84.0	78.1	-142.8	164.7	16.4	8.6	6.2
116	19.4	20.2	-143.1	160.6	-139.6	160.1	-51.2	147.5	-111.8	165.1	16.6	10.7	6.2
117	20.0	155.2	-142.9	163.8	-134.8	166.2	-145.6	147.7	-128.8	70.2	19.1	3.9	6.4
118	20.3	170.4	-136.6	148.8	-88.6	65.5	-121.2	143.0	-126.6	83.3	16.1	4.4	6.3
119	20.3	-136.7	-65.1	158.5	-117.4	-85.5	-52.3	150.2	-123.8	57.2	14.1	11.9	5.5
120	20.6	20.2	-144.9	155.5	-141.8	154.1	-57.3	155.9	-120.7	72.9	15.6	9.4	6.1
121	21.0	171.3	-59.0	144.4	-145.8	155.4	-84.9	76.7	-129.0	68.0	14.8	8.8	6.0
122	22.3	162.7	-138.5	164.4	-61.4	164.2	-51.2	146.8	-125.6	71.1	17.0	13.6	6.0
123	22.5	160.0	-140.9	162.9	-142.7	160.8	-52.4	144.1	-125.6	70.4	17.8	10.8	6.3
124	23.6	89.6	-152.4	156.7	-112.3	153.4	-55.3	153.5	-120.1	73.9	15.8	9.3	6.0
125	24.1	147.4	-142.9	161.3	-141.2	159.1	-52.9	148.6	-112.8	166.3	18.4	10.1	6.4
126	25.1	164.7	-164.6	-175.4	-131.5	172.7	-51.7	145.1	-108.3	36.6	17.5	12.1	6.1

Figure S3 All the 126 CFZ conformers. Morph = N-C-C-N dihedral angle, phi and psi dihedral angles (degrees = deg) of all the residues (hPhe, Leu1, Phe, Leu2), Head-Tail, Ring-Ring distances (Å), and Radius of gyration (Å).

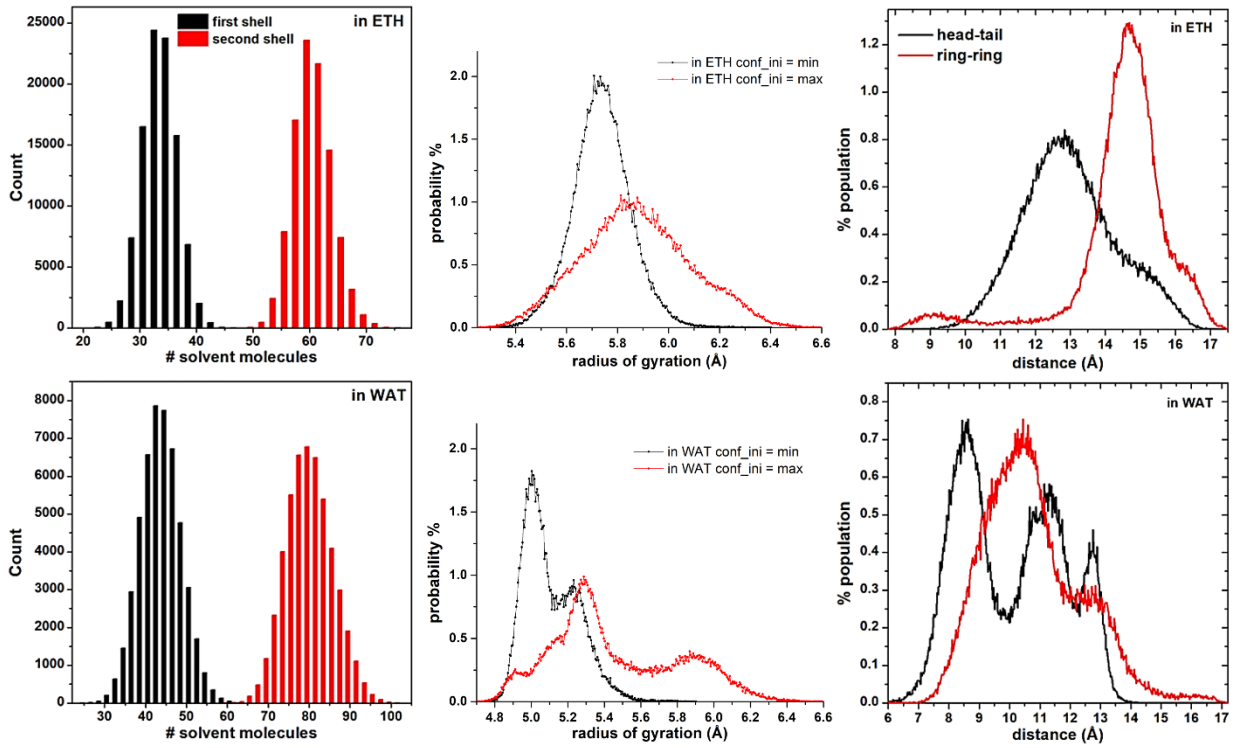

Figure S4 Radius of gyration, head-tail, and ring-ring distance plots depicting the CFZ conformations' evolution in water and ethanol solutions obtained through classical non-reactive MD simulations (AMBER16 – ff14SB and gaff force fields). The distributions of the number of solvent molecules in the first (within 2.8 Å) and second (within 3.5 Å) solvation shells are also displayed.

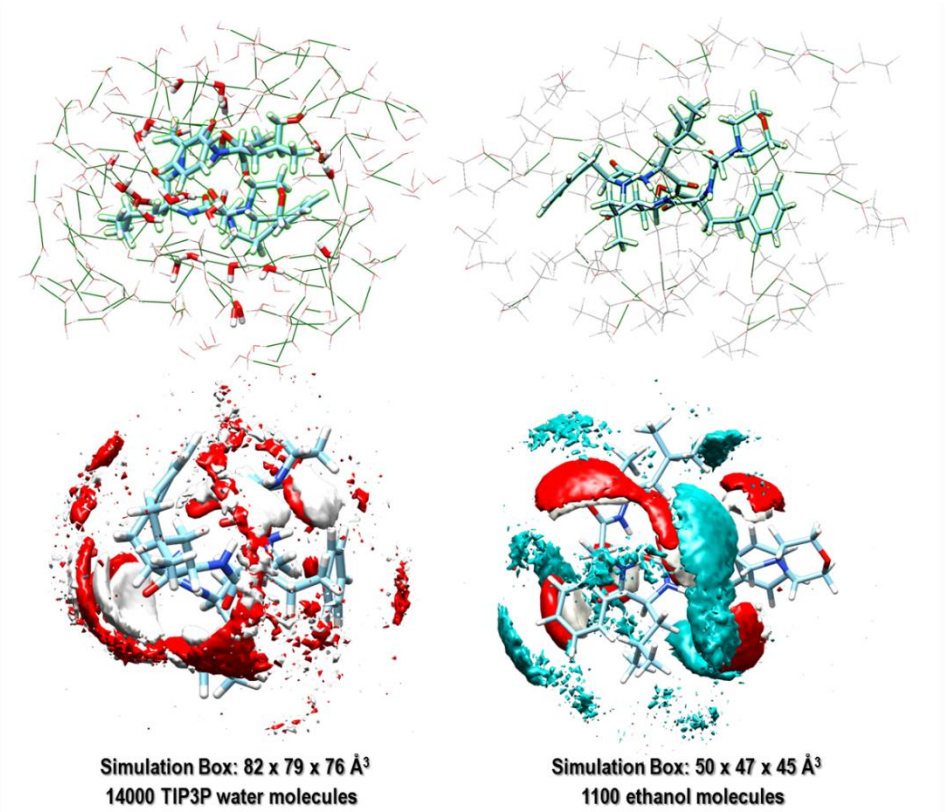

Figure S5 CFZ molecules surrounded by water (left) and ethanol (right) molecules (hydrogen bond = green lines). Spatial density distribution of the solvent atoms around an average representative structure of CFZ calculated from the last portions of the trajectories. Density regions: red = water and ethanol oxygens, white = water H and ethanol H(OH). Cyan = ethanol H(CH3).

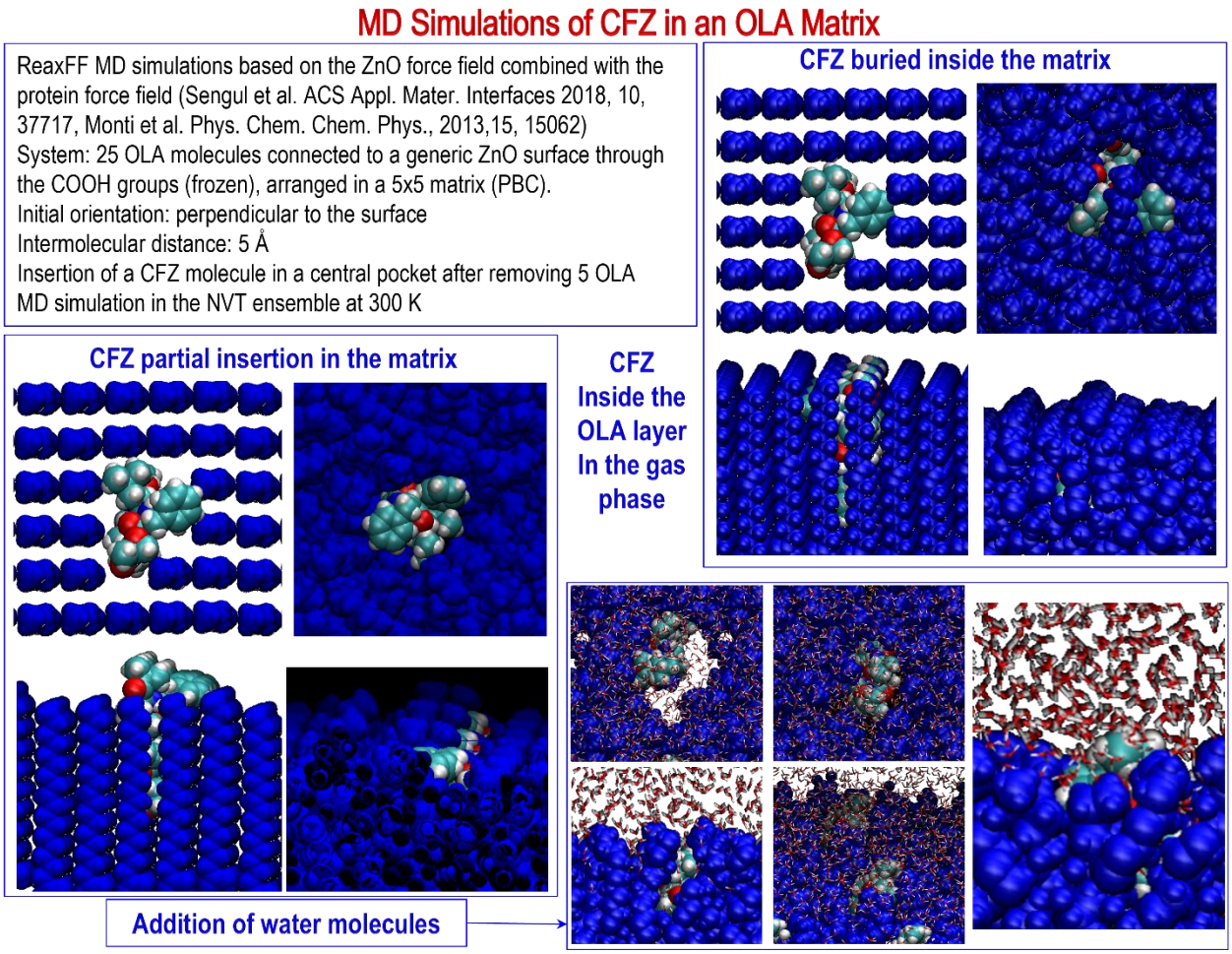

Figure S6 OLA matrix model with and without solvent molecules. Blue vdW spheres represent OLA. Without solvent, the OLA chains tend to entrap the drug by closing the pocket's opening.

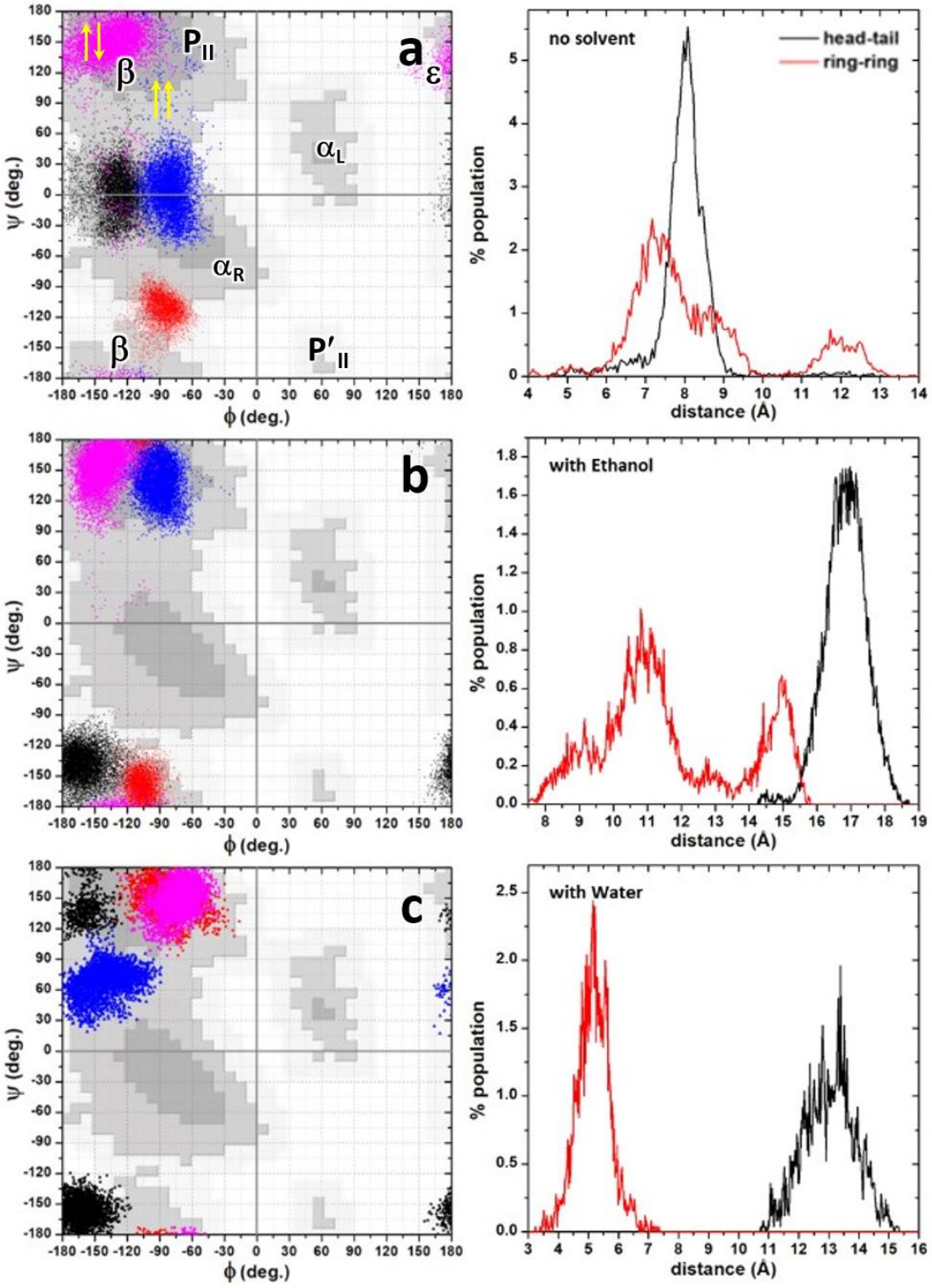

Figure S7 Ramachandran plots and respective head-tail and ring-ring distances of CFZ in the OLA matrix pocket without solvent molecules (a) in ethanol (b) and in water (c).

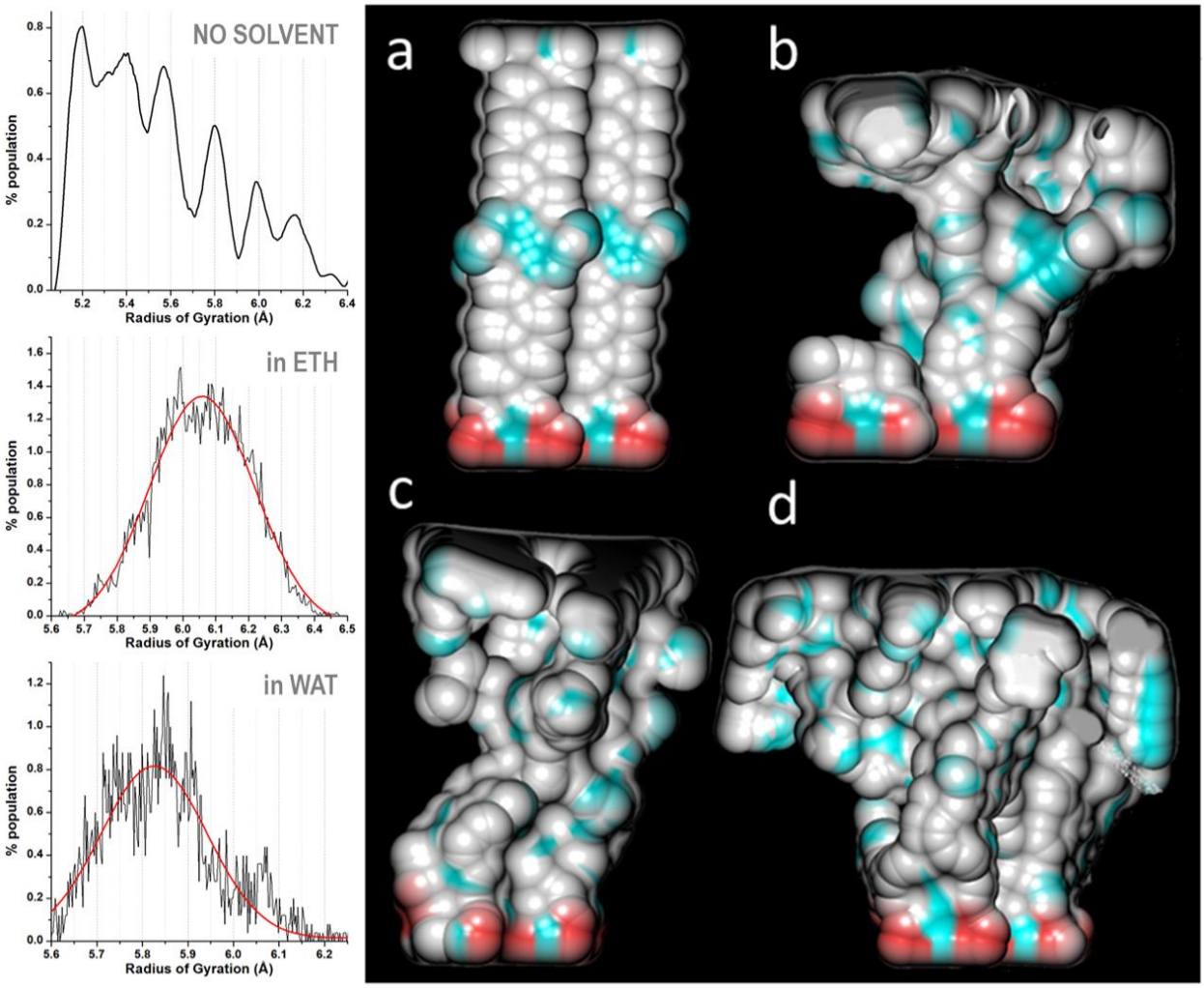

Figure S8 Distributions of the Radius of gyration of CFZ in the OLA matrix pocket without solvent, in ethanol, and water. Volume of the initial (a) and final (b, c, d) binding pockets without solvent (b), in ethanol (c) and water (d). The pocket volume has been obtained by using the CAVER Analyst 2.0 (BETA 2) software (Jurcik, A., Bednar, D., Byska, J., Marques, S. M., Furmanova, K., Daniel, L., Kokkonen, P., Brezovsky, J., Strnad, O., Stourac, J., Pavelka, A., Manak, M., Damborsky, J., Kozlikova, B.: CAVER Analyst 2.0: Analysis and Visualization of Channels and Tunnels in Protein Structures and Molecular Dynamics Trajectories., Bioinformatics, bty386, 2018).

The pocket volume is mapped through a combination of spheres with different radii. The color of the spheres depends on the contributing atoms (H white, C cyan, O red).

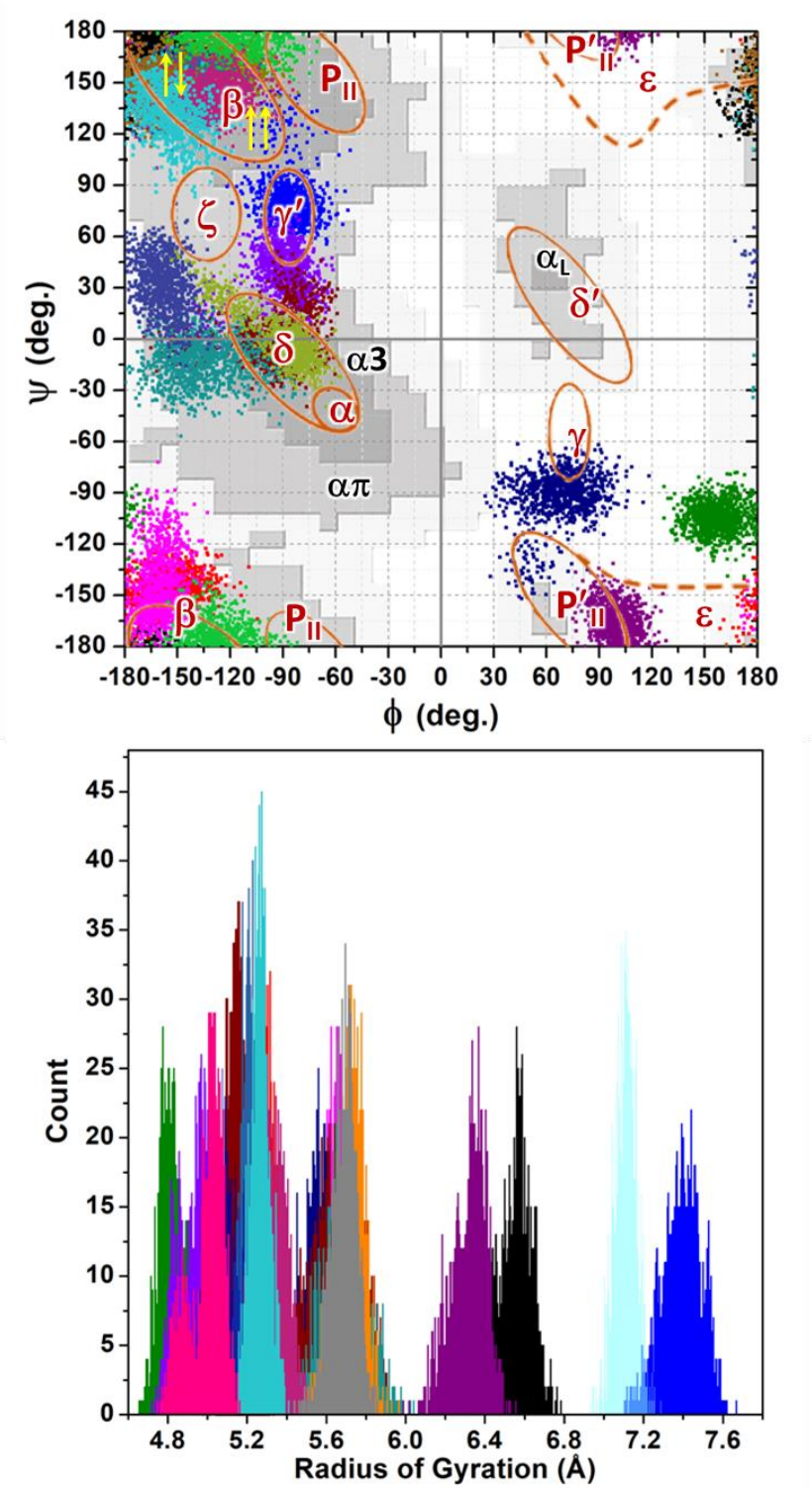

Figure S9 Top. Ramachandran plot of the CFZ molecules adsorbed on the OLA-functionalized ZnONP. Following the indications of Ref. RAMACHANDRAN, we have inserted all the regions that the authors used to classify the conformation of proteins and peptides. Besides the various types of α-helix, β-strands, and collagen-like motifs, already observed in the other Ramachandran plots describing the molecule in solution, γ-turns, γ′-turns, and ε (reflecting the somewhat extended chain of the molecules) regions are also populated due to the constraints determined by the carrier-drug association. **Bottom**. Distributions of Rgyr of CFZ adsorbed on the carrier.